RSC Advances

ROYAL SOCIETY OF CHEMISTRY

www.rsc.org/advances

Cite this: DOI: 10.1039/c0xx00000x

www.rsc.org/xxxxxx

ARTICLE TYPE

Photosensitive polyoxometalate-induced formation of thermotropic liquid crystal nanomaterial and its photovoltaic effect †

Jian-Sheng Li,‡[a] Xiao-Jing Sang,‡[a] Wei-Lin Chen,*[a] Rong-Lin Zhong,[a] Ying Lu,*[a] Lan-Cui Zhang,[b] Zhong-Min Su,[a] and En-Bo Wang*[a]

Received (in XXX, XXX) Xth XXXXXXXXX 200X, Accepted Xth XXXXXXXXX 200X
DOI: 10.1039/b000000x

The photosensitive polyoxometalate (POM) $[PW_{11}O_{39}RhCH_2CO_2H]^{5-}$ was firstly introduced into the liquid crystal material through the encapsulation of dimethyldioctadecylammonium ($DODA^+$). The theoretical calculation was performed to simulate the distribution of $DODA^+$ around the POM anion. The surface photovoltage spectroscopy (SPS) result indicated that the hybrid exhibits the photovoltaic effect upon optical illumination and displays the character of a *p*-type material, which paves a new way for their potential application in the optoelectronics.

In the past few decades, polyoxometalates (POMs) have been attracting extensive interest in the field of supramolecular chemistry[1] because of their promising application as building blocks for constructing multifunctional organic-inorganic hybrid materials owing to their wealthy topologies[2] and versatility[3]. Liquid crystals are a class of fascinating fluid matter with an orderly orientation via self-assembly of molecular or other entities.[4] POM-based liquid crystal materials have been widely studied because of their potential to obtain novel functional materials owing to the synergistic properties of POM clusters and the organized structure of liquid crystals,[5] and great progress has been achieved in both the synthesis methodology and correlation revelation between the function and component structure for POM-based liquid crystal compounds.[6]

Recently, the photovoltaic effect has aroused increasing attention due to the increasingly prevalent photovoltaic power system.[7] The photovoltaic effect of liquid crystals involves the process that the nematic or smectic liquid crystals sandwiched between two plates of conductive glasses produce electromotive force upon light stimulation. Such phenomenon is extremely attractive not only in the biological liquid crystals, such as the process of detecting light signal by the visual pigment molecules in the human retina, but also in the application of high-density data storage.[8] In this field, much attention has been paid to investigate the porphyrin-based liquid crystals.[9] Nevertheless, no research has been reported about the photovoltaic effect of POM-based liquid crystals, although the excellent photoelectrical properties of POMs are mostly likely to induce the photovoltaic effect of liquid crystal materials. Hence, the design and construction of photoelectrical functionalized liquid crystal material built from specific POMs should be a promising research field.

In our previous report, we investigated the photosensitivity of $[(CH_3)_4N]_5[PW_{11}O_{39}RhCH_2CO_2H]$ that can perform photoelectric conversion upon light illumination.[10] In this communication, two new surfactant-encapsulated POM organic-inorganic hybrids $[DODA]_5[PW_{11}O_{39}RhCH_2CO_2H]$ $28H_2O$ (**1**), and $\{[CH_3(CH_2)_6]_4N\}_5[PW_{11}O_{39}RhCH_2CO_2H]$ $6H_2O$ (**2**) were obtained through the ion metathesis reaction and characterized through FTIR spectra, TG analysis and ^1H NMR spectra (Figs. S1-S6, ESI†). The obtained compound **2** is soluble in most of the organic solvent including dichloromethane, trichloroethylene, ethanol, methanol, N,N-dimethylformamide, dimethyl sulfoxide and acetone but insoluble in water, while compound **1** is only soluble in dichloromethane and trichloroethylene. **1** presented a novel kind of thermotropic liquid crystal material which could induce photovoltage and photocurrent upon light stimulation because of the excellent photoelectric properties of $[(CH_3)_4N]_5[PW_{11}O_{39}RhCH_2CO_2H]$. Here, the photosensitive POM $[PW_{11}O_{39}RhCH_2CO_2H]^{5-}$ was firstly introduced into liquid crystalline materials. Unfortunately, the mesomorphism phenomenon of **2** was not observed under our experimental condition. Nevertheless, it is worth noting that **2** presented a viscous state at room temperature and could be regarded as a novel kind of POM-based ion liquid because its phase transition temperature was below 100 °C. This work provides a new exciting opportunity for the photoelectrical functionalization of liquid crystal materials.

The thermal properties of **1** were investigated by differential scanning calorimetry (DSC), polarized optical microscopy and variable temperature X-ray diffraction (VT-XRD). The phase transition temperature, enthalpies and assignments of the phase transition are summarized in Table S1 (ESI†). As can be seen from the DSC curve in Fig. 1a, the compound **1** experienced three phase transitions below 50°C during the second heating process, in which the former two peaks were assigned to the transitions between different phases of the solid state because of the change of the layer spacing (Fig. S7, ESI†) and the third peak at 36 °C could be ascribed to the transition between solid 3 and the liquid crystal phase. The result implied that **1** could exhibit the liquid crystal phase at room temperature. The transition from the liquid crystal phase to the isotropic phase was not clearly observed during the heating process. However, the peak corresponding to the transition from the isotropic phase to the liquid crystal phase could be obviously observed at 143 °C during the first cooling process. The polarized optical microscopy image of **1** at 71 °C (Fig. 1b) revealed the appearance of a birefringent fluid with a fan-shaped texture, indicating the formation of a smectic A (SmA) phase.[11] The VT-XRD result supports the assignment of the mesophase. As shown in Fig. 1c, the three equidistant peaks at small angles at 30 °C confirmed the formation of a layer structure

in the solid state with the layer distance of 4.41nm calculated from the Bragg equation. As the temperature increases to 65 °C, the equidistant diffractions in the small-angle region could still be clearly observed with the layer distance becoming 3.72 nm. Besides, a diffuse peak appeared centering at $2\theta \approx 20^{o}$ in the wide-angle region, indicating the formation of the lamellar structure, which confirmed the identification of SmA phase by the texture. Actually, Considering the diameter of $[PW_{11}O_{39}RhCH_2CO_2H]^{5-}$ is about 0.9nm and the normal length of $DODA^{+}$ is 2.25nm, the theoretical thickness of a single compound **1** should be 5.4nm. In consequence, the distance of the two neighboring layer (d=3.72 nm) from XRD measurement at 65 °C is $(L_{DODA}{}^{+} + L_{POM}) < d < (2L_{DODA}{}^{+} + L_{POM})$. Therefore, the alkyl chains are partially interdigitated or tilted in the smectic phase. A possible packing structure of compound **1** is shown in Fig. 1d. TEM image (Fig. 1e) shows that **1** is assembled into an irregular spherical shape with the diameter of about 800 nm by sheet piling from a mixed solvent (volume of chloroform / ethanol = 1:2) and they could maintain stable even when free of solvent. The local magnified image (Fig. 1f) confirmed the lamellar structure of **1** and the layer spacing was estimated to be 4.45nm which is very close to the result of VT-XRD (4.41nm).

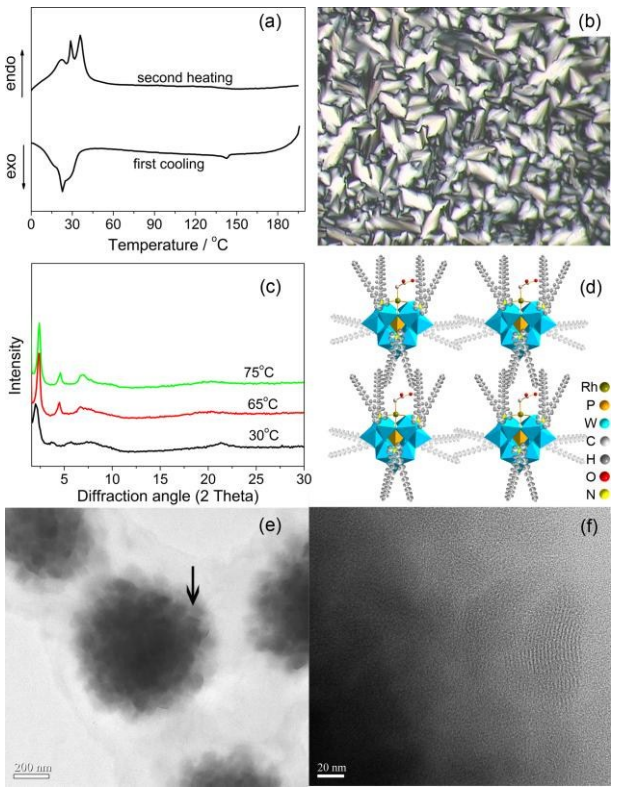

Fig. 1 a) DSC curve of **1**; b) Polarized optical microscopy image for **1** at 71°C during the cooling process; c) VT-XRD patterns of **1**; d) Schematic drawing of packing model for **1**: olive, Rh; orange, P; cyan, W; light grey, C; dark grey, H; red, O; yellow, N; e) TEM image of **1** from a mixed solvent (chloroform/ethanol = 1:2) and f) magnified image of the local region in (e) indicated by an arrow.

To further understand the arrangement structure of the surfactant around the POM anion, the electrostatic potential map of $[PW_{11}O_{39}RhCH_2CO_2H]^{5-}$ was simulated through the theoretical calculation to present the distribution of its negative charge. According to previous reports, a hybrid meta exchange-correlation functional named M06 is recommended by Truhlar and co-workers for calculation applications involving organometallic and inorganometallic chemistry.[12] All species here were calculated with M06 hybrid functional. The structure was optimized at the presence of within the nonequilibrium polarizable continuum model (PCM)[13] approach simulating the solvent effect (chloroform). Taking into account the relativistic effect for transition-metal ion, the effective core potential (ECP)[14] double-ζ(DZ) basis set of LanL2DZ is applied to the W and Rh atoms and the 6-31G* basis set is used for the nonmetal atoms. Fig. 2 displays the simulated electrostatic potential map of $[PW_{11}O_{39}RhCH_2CO_2H]^{5-}$ according to its optimized structure (Fig. S8, ESI†). The red region on the electrostatic potential map is relative negative, which means the negative charge is mainly distributed in the bridge-oxygen atoms. Besides, more negative charge is distributed in the bridge-oxygen atoms around the transition metal Rh. In consequence, we speculated that more $DODA^{+}$ cations were arranged around the Rh atom rather than W atoms, just as shown in Fig. 1d.

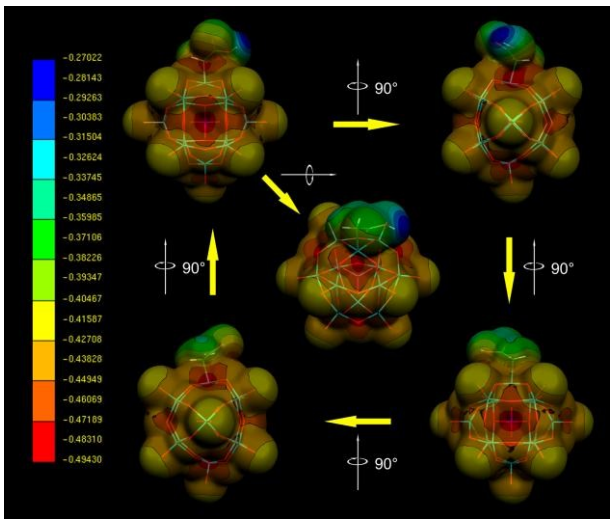

Fig. 2 The electrostatic potential map of $[PW_{11}O_{39}RhCH_2CO_2H]^{5-}$ shown from the different directions.

The thermal properties of **2** were studied by DSC measurement (Fig. S9, ESI†), showing that it can process the phase transformation from the solid state to the isotropic phase at 73 °C. For this reason, compound **2** can be assigned as a novel kind of ionic liquid.[15]

The surface photovoltage spectroscopy (SPS) was carried out to detect the photovoltaic effect of **1**. The surface photovoltage represents the change of the surface potential barrier of the measured materials upon light illumination.[16] It is known that excitation of POMs usually promotes the electron transition from the highest occupied molecular orbitals (HOMOs) to the lowest unoccupied molecular orbitals (LUMOs), which is analogous to the electron transition process from the valence band (VB) to the conduction band (CB) in the semiconductor.[17] The charge transfer process could be investigated through SPS spectra. Fig. 3a was the UV-vis absorption spectra of **1** in chloroform solution. It is obvious that **1** exhibits two absorption bands in the range of 300-600 nm, which can be assigned to the O→M charge transition band. Referred to the absorption spectra, the SPS response of **1** displayed the similar transition band from 300 nm to 600 nm except a steep drop below 327 nm due to the self-absorption of ITO electrodes, demonstrating that the electron transition in **1** contributed to the SPS response. Furthermore, the electric-field-induced surface photovoltaic spectroscopy (EFISPS) of **1** was performed to show the changes of its SPS response in different external electric fields. As can be seen from Fig. 3b, the

SPS response of **1** increased when a positive external voltage was applied. Alternatively, a negative external electric field resulted in the weaker SPS responses, and even in the reverse direction. These results implied that compound **1** takes the character of a *p*-type material because the direction of the built-in field for the p-type material coincides with that of a positive external electric field, which could enhance the separation of the photogenerated electron-hole pairs and accordingly increase the SPS response.[18] Further, the EFISPS of $[(CH_3)_4N]_5[PW_{11}O_{39}RhCH_2CO_2H]$ was investigated for comparison (Fig. 3c). It can be concluded that $[(CH_3)_4N]_5[PW_{11}O_{39}RhCH_2CO_2H]$ exhibited similar photovoltaic effect with compound **1** upon illumination and displayed the character of a p-type material under effect of external electric fields. This result indicated that the photovoltaic effect of **1** was originated from the POM anion, which was consistent with the analysis of UV-vis spectra. The photoelectrical conversion of **1** was further detected by the photocurrent-time curve (Fig. 2d), which was recorded through illuminating the sample under the simulated AM1.5 solar illumination. A homemade simple device with the sandwich structure of FTO-sample-FTO was constructed for the photocurrent measurement. The result demonstrated that **1** could produce the photocurrent under simulated sunlight. Further, there was almost no decrease for the photocurrent after the measurement for 600 s. This phenomenon implied that the as-prepared POM-based liquid crystal material could perform photoelectric conversion under solar light.

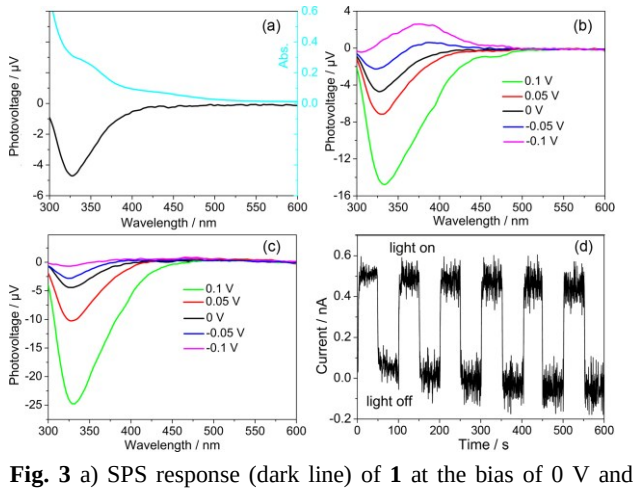

Fig. 3 a) SPS response (dark line) of **1** at the bias of 0 V and UV-vis absorption spectra (cyan line) for **1**; EFISPS responses for: b) **1**; c) $\{PW_{11}Rh\}$ and d) the photocurrent-time curve of the device containing FTO-**1**-FTO during light switching on/off.

In conclusion, the photosensitive POM $[PW_{11}O_{39}RhCH_2CO_2H]^{5-}$ was firstly employed as the building block to construct two organic-inorganic hybrids (**1** and **2**). **1** shows the characteristic thermotropic liquid crystal behavior. Moreover, its photovoltaic properties was explored for the first time. The property combined with the liquid crystalline phase and photosensitivity of the polyoxoanion makes this hybrid material of great potential in areas ranging from biology, photoelectric memory storage, switch to solar cells. **2** presents a novel kind of POM-based ionic liquid. This work provides a new strategy for constructing photoelectric functional liquid crystal materials. Further study will focus on exploring the possible application in photovoltaic cells of these hybrids.

This work was financially supported by the National Natural Science Foundation of China (No. 21131001 and 21201031), Ph. D station Specialized Research Foundation of Ministry of Education for Universities (No. 20120043120007), Science and Technology Development Project Foundation of Jilin Province (No. 201201072), the foundation of China Scholarship Council, and the Analysis and Testing Foundation of Northeast Normal University.

Notes and references

[a] *Key Laboratory of Polyoxometalate Science of Ministry of Education, Department of Chemistry, Northeast Normal University, Changchun, Jilin 130024. E-mail: wangeb889@nenu.edu.cn; chenwl@nenu.edu.cn.*
[b] *School of Chemistry and Chemical Engineering, Liaoning Normal University, Dalian 116029.*

† Electronic Supplementary Information (ESI) available: Details of the synthesis, IR, TGA, ^{1}H NMR spectra of compound **1** and **2**, DSC curve of **2**, CV curve of **1**. See DOI: 10.1039/b000000x/

‡ These authors equally contributed to this communication.

1. (a) Y. Yang, B. Zhang, Y. Wang, L. Yue, W. Li and L. Wu, *J. Am. Chem. Soc.*, 2013, **135**, 14500-14503; (b) J. E. Houston, A. R. Patterson, A. C. Jayasundera, W. Schmitt and R. C. Evans, *Chem. Commun.*, 2014, **50**, 5233-5235; (c) Y. Zhu, P. Yin, F. Xiao, D. Li, E. Bitterlich, Z. Xiao, J. Zhang, J. Hao, T. Liu, Y. Wang and Y. Wei, *J. Am. Chem. Soc.*, 2013, **135**, 17155-17160; (d) A. Di Crescenzo, L. Bardini, B. Sinjari, T. Traini, L. Marinelli, M. Carraro, R. Germani, P. Di Profio, S. Caputi, A. Di Stefano, M. Bonchio, F. Paolucci and A. Fontana, *Chem. -Eur. J.*, 2013, **19**, 16415-16423; (e) H. Wei, N. Shi, J. Zhang, Y. Guan, J. Zhang and X. Wan, *Chem. Commun.*, 2014, **50**, 9333-9335; (f) G. Modugno, Z. Syrgiannis, A. Bonasera, M. Carraro, G. Giancane, L. Valli, M. Bonchio and M. Prato, *Chem. Commun.*, 2014, **50**, 4881-4883; (g) J. Zhang, Y.-F. Song, L. Cronin and T. Liu, *Chem. -Eur. J.*, 2010, **16**, 11320-11324.
2. (a) H. Lv, J. Song, Y. V. Geletii, J. W. Vickers, J. M. Sumliner, D. G. Musaev, P. Kögerler, P. F. Zhuk, J. Bacsa, G. Zhu and C. L. Hill, *J. Am. Chem. Soc.*, 2014, **136**, 9268-9271; (b) X.-B. Han, Z.-M. Zhang, T. Zhang, Y.-G. Li, W. Lin, W. You, Z.-M. Su and E.-B. Wang, *J. Am. Chem. Soc.*, 2014, **136**, 5359-5366; (c) D. L. Long, J. Yan, A. R. Oliva, C. Busche, H. N. Miras, R. J. Errington and L. Cronin, *Chem. Commun.*, 2013,**49**, 9731-9733; (d) J. Gao, J. Yan, S. Beeg, D.-L. Long and L. Cronin, *J. Am. Chem. Soc.*, 2012, **135**, 1796-1805; (e) M. Carraro, B. S. Bassil, A. Soraru, S. Berardi, A. Suchopar, U. Kortz and M. Bonchio, *Chem. Commun.*, 2013, **49**, 7914-7916; (f) P. J. Robbins, A. J. Surman, J. Thiel, D.-L. Long and L. Cronin, *Chem. Commun.*, 2013, **49**, 1909-1911.
3. (a) S. Cardona-Serra, J. M. Clemente-Juan, E. Coronado, A. Gaita-Ariño, A. Camón, M. Evangelisti, F. Luis, M. J. Martínez-Pérez and J. Sesé, *J. Am. Chem. Soc.*, 2012, **134**, 14982-14990; (b) J. M. Maestre, X. Lopez, C. Bo, J-M. Poblet and N. Casañ-Pastor, *J. Am. Chem. Soc.* ,2001, **123**, 3749-3758; (c) C. G. Liu, W. Guan, P. Song, Z. M. Su, C. Yao, E. B. Wang, *Inorg. Chem.*, 2009, **48**, 8115-8119; (d) W. Guan, G. C. Yang, L. K. Yan and Z. M. Su, *Inorg. Chem.*, 2006, **45**, 7864−7868; (e) A. Dolbecq, P. Mialane, B. Keita and L. Nadjo, *J. Mater. Chem.*, 2012, **22**, 24509; (f) H. L. Li, S. P. Pang, S. Wu, X. L. Feng, K. Müllen and C. Bubeck, *J. Am. Chem. Soc.*, 2011, **133**, 9423-9429; (g) J. Friedl, R. Al-Oweini, M. Herpich, B. Keita, U. Kortz, U. Stimming, *Electrochim. Acta*, 2014, **141**, 357-366; (h) V. A. Grigoriev, C. L. Hill, I. A. Weinstock, *J. Am. Chem. Soc.*, 2000, **122**, 3544-3545; (i) J. Liu, H. C. Zhang, D. Tang, X. Zhang, L. K. Yan, Y. Z. Han, H. Huang, Y. Liu and Z. H. Kang, *CHEMCATCHEM*, 2014, **6**, 2634-2641; (j) Q. Han, X. Sun, J. Li, P. Ma and J. Y. Niu, *Inorg. Chem*, 2014, **53**, 6107-6112; (k) X. J. Sang, J. S. Li, L. C. Zhang, Z. J .Wang, W. L. Chen, Z. M. Zhu, Z. M .Su and E. B. Wang, *ACS Appl Mater Interfaces*, 2014, **6**, 7876-7884.
4. T. Geelhaar, K. Griesar and B. Reckmann, *Angew. Chem. Int. Ed.*, 2013, **52**, 8798-8809.
5. (a) D. G. Kurth, P. Lehmann, D. Volkmer, H. Cölfen, M. J. Koop, A. Müller and A. Du Chesne, *Chem. -Eur. J.*, 2000, **6**, 385-393; (b) S. Polarz, B. Smarsly and M. Antonietti, *Chemphyschem*, 2001, **2**, 457-461; (c) W. Li, W. Bu, H. Li, L. Wu and M. Li, *Chem. Commun.*, 2005, 3785-3787; (d) T. Zhang, C. Spitz, M. Antonietti and C. F. J. Faul, *Chem. -Eur. J.*, 2005, **11**, 1001-1009; (e) S. Yin, W. Li, J. Wang and L. Wu, *J. Phys. Chem. B*, 2008, **112**, 3983-3988.

6. (a) A. S. Poulos, D. Constantin, P. Davidson, M. Imperor, B. Pansu, P. Panine, L. Nicole and C. Sanchez, *Langmuir*, 2008, **24**, 6285-6291; (b) T. Zhang, S. Liu, D. G. Kurth and C. F. J. Faul, *Adv. Funct. Mater.*, 2009, **19**, 642-652; (c) S. Yin, H. Sun, Y. Yan, W. Li and L. Wu, *J. Phys. Chem. B*, 2009, **113**, 2355-2364; (d) X. Lin, W. Li, J. Zhang, H. Sun, Y. Yan and L. Wu, *Langmuir*, 2010, **26**, 13201-13209; (e) Y. Jiang, S. Liu, S. Li, J. Miao, J. Zhang and L. Wu, *Chem. Commun.*, 2011, **47**, 10287-10289; (f) S. Yin, H. Sun, Y. Yan, H. Zhang, W. Li and L. Wu, *J. Colloid Interface Sci.*, 2011, **361**, 548-555; (g) F. Sébastien, T. Emmanuel, H. Akram, G. Laure, P. Clause and C. Emmanuel, *New J. Chem.*, 2012, **36**, 865-868; (h) Y. Jiang, S. Liu, J. Zhang and L. Wu, *Dalton. Trans.*, 2013, **42**, 7643-7650; (i) B. Li, J. Zhang, S. Wang, W. Li and L. Wu, *Eur. J. Inorg. Chem.*, 2013, **2013**, 1869-1875; (j) Y. Jia, H.-Q. Tan, Z.-M. Zhang and E.-B. Wang, *J. Mater. Chem. C*, 2013, **1**, 3681-3685; (k) Y.-Q. Gao, Z.-M. Zhang, J.-Q. Shen, Y. Jia, Z.-J. Liu and E.-B. Wang, *CrystEngComm*, 2014, **16**, 6784-6789; (l) H.-L. Wu, Z.-M. Zhang, Y.-G. Li and E.-B. Wang, *RSC Advances*, 2014, **4**, 43806-43810.
7. W. Shin, T. Yasuda, G. Watanabe, Y. S. Yang and C. Adachi, *Chem. Mater.*, 2013, **25**, 2549-2556.
8. (a) S. Zhang, C. I. Pelligra, G. Keskar, J. Jiang, P. W. Majewski, A. D. Taylor, S. Ismail-Beigi, L. D. Pfefferle and C. O. Osuji, *Adv. Mater.*, 2012, **24**, 82-87; (b) M. O'Neill and S. M. Kelly, *Adv. Mater.*, 2011, **23**, 566-584; (c) C.-y. Liu, H.-l. Pan, M. A. Fox and A. J. Bard, *Chem. Mater.*, 1997, **9**, 1422-1429; (d) K. Yuan, L. Chen and Y. Chen, *J. Mater. Chem. C*, 2014, **2**, 3835-3845.
9. (a) M.-H. Qi and G.-F. Liu, *Chemphyschem*, 2003, **4**, 605-608; (b) M.-H. Qi and G.-F. Liu, *J. Mater. Chem.*, 2003, **13**, 2479-2484; (c) M.-H. Qi and G.-F. Liu, *J. Phys. Chem. B*, 2003, **107**, 7640-7646; (d) E.-J. Sun, Z.-Y. Sun, M. Yuan, D. Wang and T.-S. Shi, *Dyes. Pigments*, 2009, **81**, 124-130.
10. J. -S. Li, X. -J. Sang, W. -L. Chen, L. -C. Zhang, Z. -M. Su, C. Qin and E. -B. Wang, *Inorg. Chem. Commun.*, 2013, **38**, 78-82.
11. (a) S.-Y. Yin, W. Li, J.-F. Wang, L.-X. Wu, *J. Phys. Chem. B*, 2008, **112**, 3983-3988; (b) R. Steinsträsser and L. Pohl, *Angew. Chem. Internat. Edit.*, 1973, 12, 671-630.
12. (a) Y. Zhao, N. E. Schultz, D. G. Truhlar, *J. Chem. Theory Comput.*, 2006, ***2***, 364-382; (b) G. Sini, J. S. Sears, J. L. Brédas, *J. Chem. Theory Comput.*, 2011, **7**, 602-609; (c) Y. Zhao, D. Truhlar, *Theor Chem Acc*, 2008, **120**, 215-241; (d) Y. Zhao, D. G. Truhlar, *Acc. Chem. Res.*, 2008, **41**, 157-167.
13. (a) M. Cossi, G. Scalmani, N. Rega, *J. Chem. Phys.*, 2002, **117**, 43-54; (b) M. Cossi, N. Rega, G. Scalmani, V. Barone, *J. Comp. Chem.*, 2003, ***24***, 669-681; (c) D. M. Chipman, *J. Chem. Phys.*, 2000, **112**, 5558-65; (d) E. Cancès, B. Mennucci, *J. Chem. Phys.*, 2001, 114, 4744-4745; (e) S. Miertuš, E. Scrocco, J. Tomasi, *Chem. Phys.*, 1981, **55**, 117-29.
14. P. J. Hay, W. R. Wadt, *J. Chem. Phys.*, 1985, **82**, 270-83.
15. (a) P. G. Rickert, M. R. Antonio, M. A. Firestone, K.-A. Kubatko, T. Szreder, J. F. Wishart and M. L. Dietz, *J. Phys. Chem. B*, 2007, **111**, 4685-4692; (b) X. Wu, X. Tong, Q. Wu, H. Ding and W. Yan, *J. Mater. Chem. A*, 2014, **2**, 5780-5784; (c) P. G. Rickert, M. R. Antonio, M. A. Firestone, K.-A. Kubatko, T. Szreder, J. F. Wishart and M. L. Dietz, *Dalton. Trans.*, 2007, 529-531.
16. (a) J. Zhang, D. Wang, Y. Chen, T. Li, H. Mao, H. Tian, Q. Zhou and H. Xu, *Thin Solid Films*, 1997, **300**, 208-212; (b) T. Jiang, T. Xie, W. Yang, L. Chen, H. Fan and D. Wang, *J. Phys. Chem. C*, 2013, **117**, 4619-4624; (c) L. Chen, S. Li, Z. Liu, Y. Lu, D. Wang, Y. Lin and T. Xie, *Phys. Chem. Chem. Phys.*, 2013, **15**, 14262-14269.
17. A. Hiskia, A. Mylonas and E. Papaconstantinou, *Chem. Soc. Rev.*, 2001, **30**, 62–69.
18. X. Tengfeng, W. Dejun, Z. Lianjie, W. Ce, L. Tiejin, Z. Xueqin and W. Mang, *J. Phys. Chem. B*, 2000, **104**, 8177-8181.

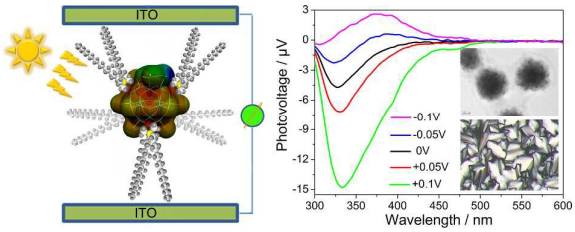

The photosensitive POM $[PW_{11}O_{39}RhCH_2CO_2H]^{5-}$ was firstly introduced into the liquid crystal nanomaterial and simulated by theoretical calculations. It exhibits the photovoltaic effect with the character of a *p*-type material.